Appl. Phys. B (2017) 123:158
DOI 10.1007/s00340-017-6734-7

Applied Physics B
Lasers and Optics

UV laser-induced poling inhibition in proton exchanged $LiNbO_3$ crystals

G. Zisis[1] · M. Manzo[2] · K. Gallo[2] · E. Soergel[3] · S. Mailis[1]

Received: 1 March 2017 / Accepted: 19 April 2017

Abstract The applicability of the UV laser-induced poling inhibition method for ferroelectric domain engineering in proton exchanged lithium niobate planar waveguides is investigated. Our results indicate that intense UV irradiation of proton exchanged lithium niobate samples can, indeed, produce poling inhibited domains in this material under certain irradiation conditions. However, there is strong indication that the temperature gradient that is formed during UV irradiation modifies the local proton concentration leading to changes in the refractive index profile of the original planar waveguide.

1 Introduction

Ferroelectric domain engineering [1] in lithium niobate (LN) is utilized in a variety of applications such as wavelength conversion by quasi-phase-matching [2] (QPM), acousto-optic devices [3], and surface/bulk micro-structuring [4]. Domain inversion in LN is commonly achieved by electric field poling (EFP) where an external electric field, which exceeds the crystals coercive field E_c, is applied along the polar direction [5] at room temperature. However, poling of fine periodic domain structures (Λ <5–6 μm) corresponds the large domain aspect ratio that leads to distortion of the ideal domain shape and size thus making fabrication of fine domains challenging [3].

Poling inhibition (PI) induced by UV laser irradiation [6, 7] in congruent (CLN) and MgO-doped LN can overcome the limitation of EFP by reducing the aspect ratio of the inverted domains allowing for the fabrication of finer domain structures. This method is capable of producing domains with a moderate depth (a few microns below the surface) that can be controlled, to some extent, by the UV laser exposure [8]. UV laser irradiation of the +z polar surface of the crystal results in a local increase of the coercive field by causing migration of lithium ions due to (1) diffusion in the temperature gradients [9] and (2) drift in the pyro-electric field[10]. Consequently, a uniform electric field applied along the z direction will invert the inherent polarisation of the crystal everywhere apart from the volume that has been affected by the UV laser irradiation, which remains poling inhibited. The depth of the PI domains suggests that such structures will be suitable for optical waveguide systems; therefore, it is important to investigate whether poling inhibition is applicable with established waveguide fabrication methods.

In this paper, we are investigating the impact of the UV-induced PI procedure on proton exchanged (PE) waveguides, which are fabricated in z-cut LN substrates. Proton exchange is a well-established method for the fabrication of low-loss waveguides, which are resistive to photorefractive damage [11]. PE waveguides are formed by the replacement of lithium ions with protons from a benzoic acid melt (up to a depth of ~1 μm), which increases the extraordinary refractive index of the crystal [12, 13]. The main question that this work attempts to address is whether the UV laser irradiation will produce sufficient coercive field contrast for selective poling, as in the case of poling inhibition of undoped crystals [6, 7]. Here, we present

✉ S. Mailis
sm@orc.soton.ac.uk

[1] Optoelectronics Research Centre, University of Southampton, Southampton SO17 1BJ, UK

[2] Department of Applied Physics, KTH-Royal Institute of Technology, 106 91 Stockholm, Sweden

[3] Institute of Physics, University of Bonn, Wegelerstrasse 8, 53115 Bonn, Germany

Published online: 27 April 2017

experimental evidence, which shows that the UV laser irradiation, indeed, produces a coercive field contrast, thus producing PI domains. However, there is strong indication that the coercive field modulation is accompanied by a change of the local proton concentration, thus modifying the original PE waveguide structure.

2 Results and discussion

2.1 Sample preparation

A set of proton exchanged samples were prepared using congruent and Mg-doped LN substrates by annealed proton exchange (APE). Most of these samples were prepared to support optical waveguide modes in the visible spectral range. The APE planar waveguides were produced by immersing LN substrates in pure benzoic acid at 200 °C for 3.5 h resulting in the replacement of lithium ions by protons from the molten benzoic acid increasing the extraordinary refractive index. The reduction of the optical nonlinearity and the spontaneous polarisation, which can be induced by direct PE in pure benzoic acid (β-phase $H_xLi_{1-x}NbO_3$), was subsequently restored by annealing in air at 325 °C for 26 h, forming a final graded-index APE waveguide with estimated $1/e$ depth of $\sim$3.1 μm, suitable for photonic applications. However, even after annealing, some residual damage remains within a submicron surface layer [14].

The samples were exposed to UV laser radiation by scanning the samples in front of a focussed laser beam resulting in linear irradiated tracks. A continuous wave UV laser beam from a frequency doubled argon ion laser (244 nm) was used in these experiments, focused to a beam radius of $\approx$2.5 μm on the +z-face of the crystal. The tracks were aligned along the crystallographic y-direction using a set of computer controlled two axes translation stage (Aerotech ABL1500). The scanning speed was kept at 0.1 mm/s. The laser powers, which were used in our experiments, were within the range of 15–37 mW, corresponding to peak intensities in the range of 0.13–0.36 MW/cm^2.

After UV irradiation, the crystals were uniformly domain inverted by electric field poling (EFP) at room temperature to complete the domain formation process. The previous PI experiments in CLN suggest that good quality, continuous PI domains can be obtained by maintaining a slow domain wall velocity during the EFP step [10]. The domain wall velocity can be controlled by the amplitude of the applied voltage [15]. In our experiments, the amplitude of the applied voltage was ramped up slowly (5 Volts/s) up to reach an electric field value of around of 19.5 kV/mm $\pm$ 100 V/mm where domain nucleation started to occur. The transparent holder which is used in our poling apparatus enables the real-time monitoring of nucleation events and domain wall movements by taking advantage of the stress induced birefringence that occurs at the domain wall.

2.2 Poling inhibition in PE:CLN

The depth profiles of the PI domains were investigated in detail using scanning electron microscopy (SEM). To reveal the ferroelectric domain topography, the poled samples were briefly etched ($\approx$1 min) in HF acid, which is known to reveal ferroelectric domains by differential etching of crystal faces with opposite polarity. Before etching, the samples were wedge-polished at an angle of $\approx$5° with respect to the laser irradiated surface resulting to a stretching of the depth profile by a factor of $1/\tan(5°) = 11.43$, which subsequently enables the detailed observation of the cross section topography. A further advantage of wedge polishing is that the surface offered to the acid has a substantial z-face component which provides very high contrast due to significant differential etching as compared to the etching [16] of a pure y-face that would take place without the wedge polishing. Finally, the large surface area, which corresponds to the wedge, is also suitable for investigation of the domain structures using piezoresponse force microscopy (PFM) due to the absence of sharp surface discontinuities.

The surface topography of a UV exposed and wedge-polished, etched PE sample is shown in the SEM images of Fig. 1. Images a, b, c, and d correspond to UV laser tracks in a PE:CLN sample, irradiated with intensities of 0.25, 0.27, 0.30, 0.31 MW/cm^2, respectively. The wedge-polished surface lies on the left of each image as indicated by the arrow, while the vertical dash line indicates the locations where the slope changes.

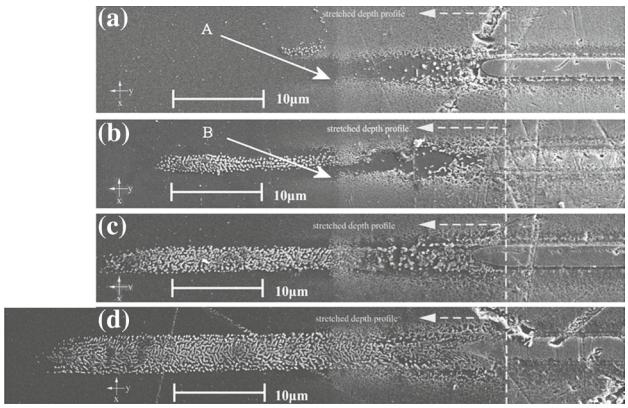

Fig. 1 SEM images of wedge-polished and HF-etched tracks fabricated UV-laser irradiation followed by EFP. The laser intensities used are: **a** 0.25 MW/cm^2, **b** 0.27 MW/cm^2, **c** 0.30 MW/cm^2, and **d** 0.31 MW/cm^2. The *white dashed lines* indicate the boundary where the slope changes due to wedge polishing. The *arrows* A and B indicate areas where the etch revealed that roughness has expanded deeper into the crystal as a result of the laser irradiation

Etch-resistant features, attributed to poling inhibition, can be observed in the SEM images of Fig. 1. In the same images, a well-defined zone of increased surface roughness (revealed after etching) can also be observed. This zone extends from the surface (indicated by the white dashed line) to a depth of approximately ≈1.7 μm, well within the proton rich volume of the crystal, which according to the fabrication conditions of this particular sample reaches a 1/e depth distribution of protons of 3 μm. It is reasonable to assume that this rough zone, the texture of which seems to be modified under the laser irradiated tracks, is associated with the concentration of protons. The etch-revealed roughness zone is likely due to crystal disorder that is associated with proton exchange at similar depth that was observed here, as shown in [17]. The polished surface texture becomes smooth again below a depth of 1.7 μm that corresponds to a proton concentration which is lower than ~60% of the surface value.

The sequence of Fig. 1a–d shows subsurface features that were revealed after etching of the poled sample. The main observation here is that as the laser intensity increases, there is an accompanying increase in the density of the etch-resistant features, which can now be identified as isolated PI nanodomains, formed within the heat-affected volume of the crystal [10], that extends deeper from the surface with increasing irradiating laser intensity. These features are characteristic of PI domain formation. In comparison, using the same irradiation conditions in CLN crystals, it was possible to obtain solid PI domains rather than isolated nanodomains. Furthermore, changes in the etched surface texture, which can be observed in the vicinity of the laser-affected volume, indicate that the concentration of protons below the laser tracks has been modified. In the areas A and B in particular, indicated by the arrows in Fig. 1a and b, the rough textured area seems to have been extended further in to the depth of the crystal in association with the laser irradiation. A modification of the proton concentration is possible through diffusion in the temperature gradients that are formed during UV laser irradiation, which causes protons to diffuse away form the high-temperature volume to the colder periphery thus increasing the proton concentration there. Interestingly, in the lower intensity range (Fig. 1b), the etch-resistant PI features appear preferentially below the 1.7 μm-deep proton rich zone, which indicates (1) that the irradiation threshold for PI domains in the proton rich area is higher and (2) that PI domain formation is accompanied by a change in the proton concentration, which can affect the integrity of the PE waveguide as will be shown later. These observations are in accordance with the previous work, which indicates that a high concentration of protons also serves as poling inhibitor [18] and, therefore, competes with the poling inhibition effect that is caused by the laser irradiation.

In an attempt to obtain solid domains, the irradiating laser intensity was further increased to 0.36 MW/cm^2. For this higher laser intensity, a solid PI domain was formed, shown in the SEM image of Fig. 2a that is similar to the PI domains observed in CLN crystals. The ferroelectric domain nature of the PI domains was also investigated using PFM. The image, shown in Fig. 2b, reveals that the piezoresponse contrast of the feature is characteristic of a ferroelectric domain with opposite polarity with respect to the surrounding crystal volume. The PI domain that was obtained at this higher intensity levels is accompanied by significant laser-induced damage of the surface, which forms a non-ferroelectric zone corresponding to the volume of the crystal that has been subjected to the peak of the heat distribution, which is a consequence of the absorbed UV laser radiation. In the previous work [6, 7, 10], the formation of PI domains in congruent crystals was attributed to the redistribution of lithium ions under the influence of the UV laser-induced temperature gradient. In the case of the PE crystal, a similar mechanism is assumed, which, however, requires a further redistribution of protons as well as lithium ions under the same driving force of temperature gradient-based diffusion.

Wedge polishing helps revealing a stretched profile of the laser-affected volume where the PI domains are expected to form. It is possible to measure, therefore, the depths and widths of these domains from the SEM images, which are shown in Fig. 1. The plots, which are shown in Fig. 3, show the change in depth and width of the observed features as a function of the irradiating laser peak intensity. The data points are accompanied by special symbols (as explained in the legend of the figure) that provide a schematic representation of the types of features that were observed indicating the laser intensity ranges that correspond to modification of the proton concentration (below 0.25MW/cm^2), scattered nanodomains (0.25–0.31 MW/cm^2), and solid domains at 0.36 MW/cm^2, which, however, is accompanied by substantial laser-induced damage of the surface. The depth of

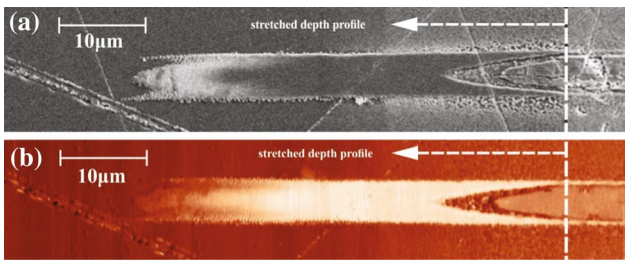

Fig. 2 SEM image (**a**) and PFM scan (**b**) of the depth profile of an UV-induced PI domain in PE sample. The UV-laser intensity used was 0.36 MW/cm^2. The *dashed lines* indicate the boundary where the slope changes due to wedge polishing

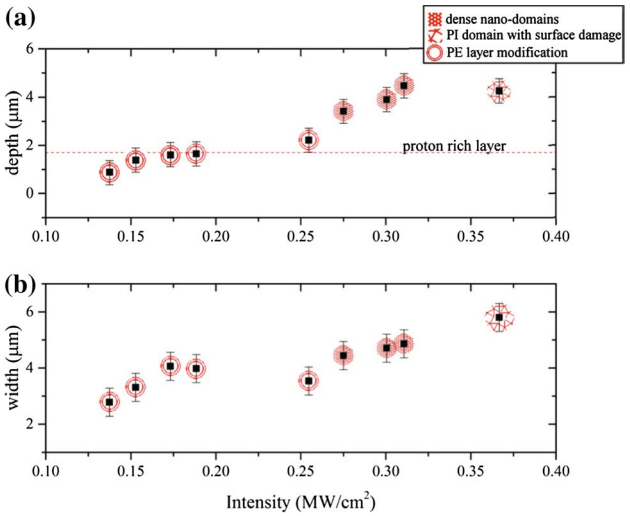

Fig. 3 Depth (**a**) and width (**b**) of UV-laser tracks in a PE undoped CLN (as measured from the SEM images of wedge-polished samples) plotted as a function of the laser intensity. The *red symbols* correspond to various surface and depth qualities and the *red dashed line* corresponds to the depth of the high proton exchange layer

the observed features increases with laser power. However, their nature changes from mere proton concentration modification through to scattered nanodomains and finally to solid domains with a maximum depth of $\sim$ 4 μm. The surface width of the laser damaged area follows a similar trend showing a monotonic behaviour as expected by the heat flow dynamics [9].

2.3 Poling inhibition in MgO-doped PE:CLN

UV laser-induced PI domains were also achieved in Mg-doped PE:CLN waveguides. An SEM image of the wedge-polished/etched cross section of a PI domain is shown in Fig. 4. Similarly to PE:CLN, the conditions for achieving solid PI domain formation correspond to relatively high laser intensity (0.36 MW/cm^2). Figure 4 shows that the solid PI domain is surrounded by a halo of dense nanodomains which are much more pronounced than the corresponding nanodomains that were observed in the undoped PE:CLN sample (Fig. 2a). Interestingly the PI domain becomes wider below the proton-rich layer ($\approx$1.4 μm) (rough zone), indicating that the PI dynamics in the case of the MgO-doped PE:CLN samples are more sensitive to the proton concentration as compared to the case of the undoped PE:CLN samples. Finally, the measured overall depth of the PI domains in Mg-doped PE:CLN was found to be similar with the PI depth measured in undoped PE:CLN, which is $\approx$4.3 μm. This result differs to the previous work on non PE samples where it was observed that Mg-doped CLN crystals produced in general shallower domains than in CLN for the same UV laser irradiation conditions [10].

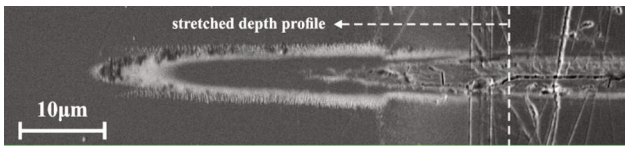

Fig. 4 SEM image of the depth profile of a UV-induced PI domain in Mg-doped PE:CLN waveguide. The UV-laser intensity used was 0.36 MW/cm^2. The *dashed lines* indicate the boundary where the slope changes due to wedge polishing

2.4 Waveguide transmission

In the previous section, it was argued that the observations of the etched cross sections suggest that the laser irradiation step modifies the local proton concentration. However, redistribution of protons should affect the PE waveguide refractive index profile. The integrity of the PE waveguide in the vicinity of the laser irradiated tracks was investigated by optical transmission experiments. The PE:CLN sample under investigation has been uniformly proton exchanged on its +z-face to form a planar waveguide that can support TM mode [12, 19]. The UV laser tracks were exposed along the *y*-direction of the crystal on the +z-face. Both y-faces of the crystal sample were edge polished after the PI process to enable endfire coupling of light into the planar PE optical waveguide. A HeNe laser (633 nm) beam was focussed by a microscope objective onto the polished edge of the PE waveguide. The near-field intensity profile of the

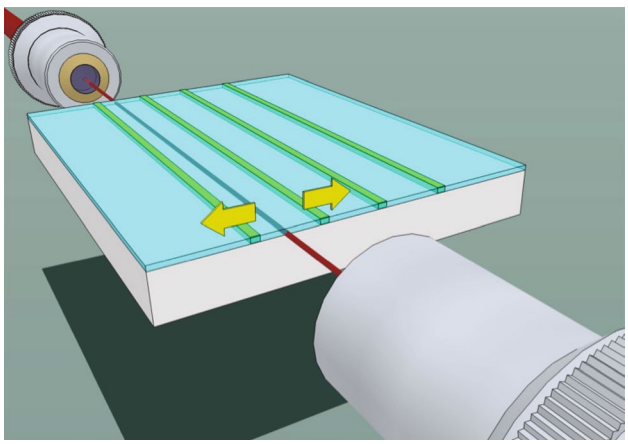

Fig. 5 Schematic of the waveguide coupling experiment. A 633 nm HeNe laser beam is coupled into the PE waveguide and coupled out through two objectives. The waveguide coupling point is able to move anywhere between the UV-laser irradiated tracks

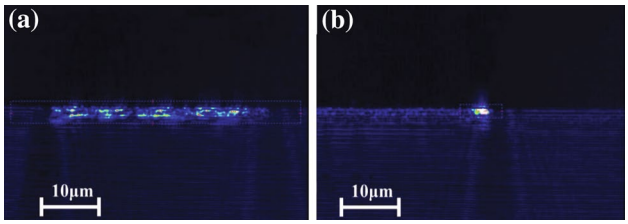

Fig. 6 Near-field intensity profiles of two UV-induced PI domains on the PE:CLN surface planar waveguide, fabricated by a UV-laser beam at intensity of 0.36 MW/cm^2 Incident coupling point of the HeNe beam is located **a** between the two adjacent irradiated tracks and **b** right of the centre of the track

propagating mode was imaged on a CCD camera using a second microscope objective. A schematic illustrating the experimental setup is shown in Fig. 5. By translating the sample, it was possible to vary the coupling position relative to the location of the UV laser tracks thus probing any changes on the propagating planar waveguide mode that were caused by the PI process in the vicinity of the UV irradiated tracks.

By monitoring the near-field mode profile at the output facet, we observed that when the coupling position lies anywhere between two adjacent laser tracks, which are separated by 100μm, the waveguide mode, shown in Fig. 6a, corresponds to that of a planar waveguide. The planar waveguide supports two modes at 633 nm which introduces variations in the vertical direction of the intensity profile. When the coupling point is located at the edge of the laser track, the mode appears to be confined both in the vertical and horizontal directions to an isolated spot close to the surface of the sample (Fig. 6b). These observations are in agreement with the hypothesis that protons are being displaced from the centre of the laser track to the periphery due to diffusion under the influence of the temperature gradient that is formed by the strong absorption of the UV laser radiation. The diffused protons, which are accumulated adjacent to the irradiated track, increase the refractive index there thus forming a channel waveguide. Moreover, no light propagation is observed when the coupling point is overlapped with the laser track, which again is in agreement with the assumed reduction in the proton concentration there. Finally, light that propagates in the 100 μm wide section of the original planar waveguide which lies between two tracks will experience lateral confinement due to the refractive index modulation that is associated with the redistribution of protons in the vicinity of the irradiated tracks. This lateral confinement accounts for the lateral intensity variation in the planar waveguide mode that can be observed in Fig. 6a.

3 Conclusions

In summary, the feasibility of using the poling inhibition method for ferroelectric domain engineering of PE lithium niobate waveguides was investigated. It was found that under specific conditions, UV irradiation can induce PI in both PE:CLN and PE:MgO:CLN waveguides as verified by domain orientation selective etching and PFM experiments. However, solid PI domains occur at higher laser intensities as compared to undoped CLN crystals, which introduces unwanted laser-induced damage of the surface of the waveguide limiting the utility of this method for domain engineering. In addition, our results strongly suggest that the UV laser irradiation of the PE crystals changes the proton concentration locally. Waveguide transmission measurements in the processed PE:CLN samples exhibited further lateral confinement of the coupled light adjacent to the irradiated tracks, indicating that protons diffuse away from the irradiated volume during the UV exposure step.

References

1. V.Y. Shur, Ferroelectrics **340**, 3 (2006)
2. G. Miller et al., Opt. Lett. **22**, 1834 (1997)
3. R.V. Schmidt, I.P. Kaminow, IEEE J. Quant. Electr. **QE11**, 57 (1975)
4. C. Sones et al., J. Micromech. Microeng. **12**, 53 (2002)
5. M. Yamada, N. Nada, M. Saitoh, K. Watanabe, Appl. Phys. Lett. **62**, 435 (1993)
6. C.L. Sones et al., Appl. Phys. Lett **92**, 072905 (2008)
7. H. Steigerwald et al., Phys. Rev. B **82**, 214105 (2010)
8. G. Zisis, C.Y.J. Ying, E. Soergel, S. Mailis, J. Appl. Phys. **115**, 124102 (2014)
9. A.C. Muir et al., Appl. Phys. A Mater. Sci. Process. **83**, 389 (2006)
10. C.Y.J. Ying, G.J. Daniell, H. Steigerwald, E. Soergel, S. Mailis, J. Appl. Phys. **114**, 083101 (2013)
11. T. Fujiwara, R. Srivatava, X.F. Cao, R.V. Ramaswamy, Opt. Lett. **18**, 346 (1993)
12. J.L. Jackel, C.E. Rice, J.J. Veselka, Appl. Phys. Lett. **41**, 607 (1982)
13. Y.N. Korkishko, V.A. Fedorov, J. Appl. Phys. **82**, 1010 (1997)
14. M. Bortz, L. Eyres, M. Fejer, Appl. Phys. Lett. **62**, 2012 (1993)
15. V. Gopalan, T.E. Mitchell, K.E. Sicakfus, Solid State Comm. **109**, 111 (1999)
16. C. Sones, S. Mailis, W. Brocklesby, R. Eason, J. Owen, J. Mat. Chem. **12**, 295 (2002)
17. S. Kostritskii et al., J. Eur. Opt. Soc. Rap. Public. **9**, 14055 (2014)
18. M. Manzo, F. Laurell, V. Pasiskevicius, K. Gallo, Appl. Phys. Lett. **98**, 122910 (2011)
19. P. Nekvindova et al., Opt. Mat. **19**, 245 (2002)